Remote Sensing Letters

ISSN: 2150-704X (Print) 2150-7058 (Online) Journal homepage: http://www.tandfonline.com/loi/trsl20

Derivation of the characteristics of the Surface Urban Heat Island in the Greater Toronto area using thermal infrared remote sensing

Chengming Ye, MinJie Wang & Jonathan Li

REMOTE SENSING LETTERS, 2017
VOL. 8, NO. 7, 637–646
http://dx.doi.org/10.1080/2150704X.2017.1312025

Derivation of the characteristics of the Surface Urban Heat Island in the Greater Toronto area using thermal infrared remote sensing

Chengming Ye[a], MinJie Wang[b] and Jonathan Li[b]

[a]Key Laboratory of Earth Exploration and Information Technology of Ministry of Education (Chengdu University of Technology), Chengdu, P.R.China; [b]Department of Geography and Environmental Management, Faculty of Environment, University of Waterloo, Waterloo, Canada

ABSTRACT

For the past decades, there have been increasing concerns about urban environmental degradation, especially under the circumstance of urbanization. This paper compares the trends between air temperature and surface temperature, and characterizes spatial distribution and connection with relevant urban characteristics, in the Greater Toronto Area (GTA) of Ontario in the context of surface urban heat island (SUHI). The trends in annual and seasonal temperature were investigated in the GTA from 1984 to 2014. A local scale investigation was continued by applying Landsat and ASTER thermal-band images in order to characterize SUHI intensity in the study area. Results show that strong SUHI phenomenon is mainly observed at downtown Toronto and industrial areas and the temperature variation is consistent with the pace of urbanization, such as low NDVI, land use change, increasing population and new roads.

ARTICLE HISTORY
Received 30 October 2016
Accepted 22 March 2017

1. Introduction

Surface Urban Heat Island (SUHI) is one term which exams the difference of land surface temperature (LST) derived from remote-sensing data (Sobrino et al. 2013) and its actuality is one important index of ecological conditions in urban areas. Constantly strengthen of extreme weather and climate events by **Urban Heat Island(UHI)** could become serious challenges for socioeconomic and natural systems, such as urban heat wave (Smargiassi et al. 2008; Curriero et al. 2002), susceptible to UHI (Semenza et al. 1996), photochemical smog (Rosenfeld et al. 1995), rainfall intensity(Dixon and Mote 2003), damage to the ecosystems and wildlife, the pollution of drinking water (Krause et al. 2004; Finkenbine, Atwater, and Mavinic 2000). There are increasing concerns about the side effect of UHI regarding to our urban environments, especially how abnormal temperature will interact with UHI (Coutts, Beringer, and Tapper 2010).

By examining long-term annual mean temperature in the Greater Toronto Area(GTA), Ontario, Canada, it is found that the increasing trend of temperature is consistent with the pace of urbanization which starts from 1920 at downtown Toronto and 1960 at the

CONTACT Chengming Ye rsgis@sina.com Key Laboratory of Earth Exploration and Information Technology of Ministry of Education (Chengdu University of Technology), 1#, Dongsanlu, Erxianqiao, Chengdu 610059, Sichuan, P.R.China

suburban areas (Mohsin and Gough 2014). With an increasing growth in the quantity and intensity of extreme heat events, and 80% of Canadians living in urban areas, for example, the GTA, there is an urgent requirement of SUHI mapping and monitoring in spite of Canada's well-known cold temperature.

The local scale climate of the GTA is fluctuated by a change in elevation from the shore of Lake Ontario. Generally, Lake Ontario will moderate the summer extreme temperature, which is the 'Lake Breeze' effect, by blowing winds from water to land (Scott and Huff 1996). Additional factors such as the scattered and emitted radiation from atmospheric pollutants to the urban area, the production of greenhouse gas and aerosol concentrations from air conditioning and refrigeration systems, as well from industrial processes and motorized vehicular traffic, have been recognized as additional anthropogenic climate factors for the UHI. Therefore, this paper explores the UHI from the role of urban development and characterizes the SUHI in the GTA, by using thermal infrared (TIR) remote sensing data from the past 30 years.

2. Study area and data

2.1. *Study area*

We selected the City of Toronto and its surrounding areas as our study area. The growing of the GTA is reflected by increasing of build-up areas and population. The City of Toronto, as the core of the GTA, is a characteristic study subject located near 44°N and along the western shore of Lake Ontario. Figure 1 shows the growing of urban areas of the GTA since 1945.

2.2. *Satellite images*

The selected Landsat-5 TM images of path 18, row 29 and path 18, row 30 were acquired from website of the US Geological Survey (USGS) in GeoTIFF format between 1984 and

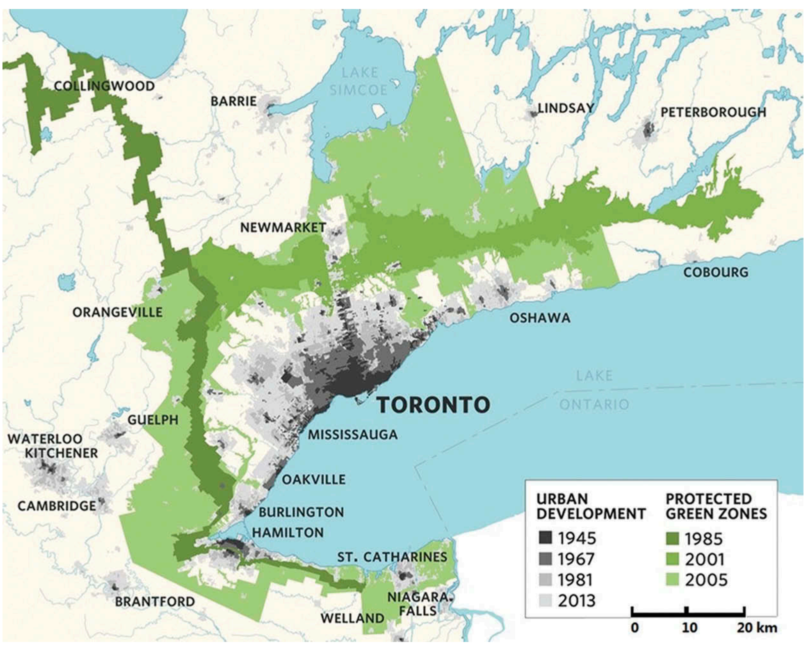

Figure 1. Change of the urban areas in the GTA.
Source: Greenbelt 2014.

2013. The raster images for each scene include 7 tiff images for 7 bands separately. Each band monitors radiance within a specific section of the light spectrum. In our study, the thermal band (Band 6) images are key research contents with 120 m pixel resolution.

2.3. *Historical climate data and supplementary data*

The weather stations data recorded from 1969 to 2014 were used in our study. The temperature data are available from Environment Canada (EC) for each station. According to raw meteorological data, annual, seasonal and monthly mean temperature series can be calculated separately. The supplementary data can be helpful when analyzing and evaluating the original data, such as GTA boundary, population, road network, and land use.

3. Method

3.1. *Data preprocessing*

The time series (once a year from 1984 to 2014) used in the trend analysis were tested for homogeneity by using the Mann-Whitney (MW) test. During the study period, certain stations may encounter problems such as missing data, change of measurement locations and update of instruments. Therefore the MW test insures the robustness and effectiveness of the data. The MW test, which is a non-parametric style test, identifies sample differences by first ranking all the combined sample contents with sequence regarding to sample means and medians. The result of MW test is stations' *p*-values(significant difference) are both larger than 0.05 and past the homogeneity test which insures the robustness and effectiveness of the data.

All images acquired at the different dates were resampled to 30 m and the study area was clipped out from mosaic images by taking a shapefile representing the GTA boundary as the base map. The workflow of our method is shown in Figure 2.

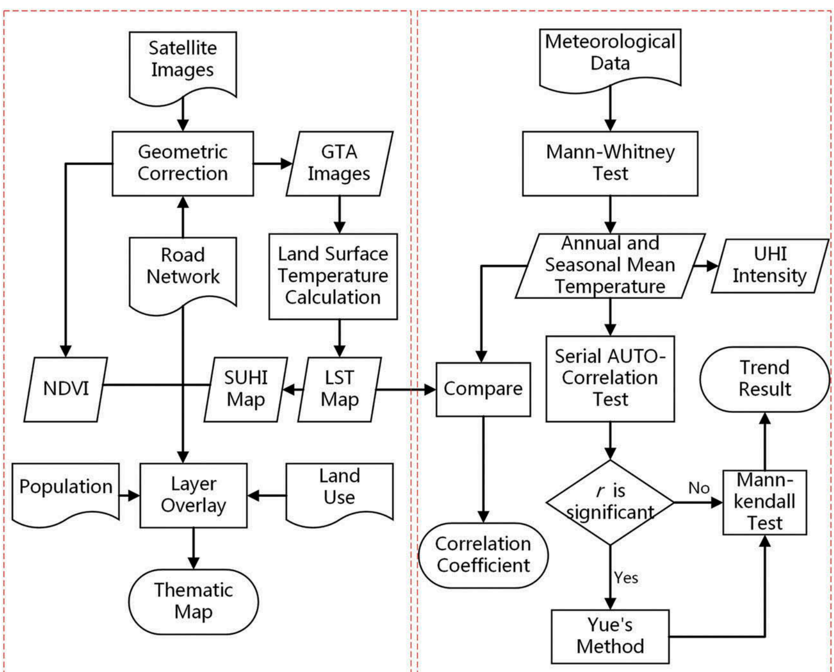

Figure 2. Flowchart of the methodology.

3.2. *Data analysis and LST estimation*

In order to reduce the effect of serial auto-correlation, the serial auto-correlation of each time series was test before applying the Mann-Kendall (MK) trend analysis. The method used to remove the time series lag-1 correlation coefficient is the autoregressive and integrated moving average (ARIMA) model. The data from the station(at Pearson International Airport) shows autocorrelation at 0.05 level for annual mean temperature and the other stations do not present autocorrelation for the data serial.

The first step for the LST conversion is to convert the digital numbers of the images to the Top of Atmosphere radiance (ToA_r) values according to spectral radiance scaling method(Eq.1). The ToAr can be calculated by:

$$ToA_r = \frac{R_{Max} - R_{Min}}{Q_{Max} - Q_{Min}} \times (DN - Q_{Min}) + R_{Min} \quad \text{(Eq.1)}$$

where R_{Max} and R_{Min} are the reference radiance extremums for each band correspondingly from metadata file. Q_{Max} and Q_{Min} are equal to the extremums of digital number to store cell value. DN is the known digital number per pixel and ToA_r is the calculated the ToAr values per cell. For Landsat-5 TM, data are stored by 8-bit pixel values which means the corresponding Q_{Max} is 255 (Q_{Max} = 65,535 for 16-bit Landsat-8 data). Eq. 1 can be further simplified as a gain and bias method in Eq.2:

$$ToA_r = (Gain \times DN) + Bias \quad \text{(Eq.2)}$$

where:

Gain = $\frac{R_{Max} - R_{Min}}{Q_{Max}}$ and Bias = R_{Min}

Next step is to calculate the LST value using the following inverse Planck function, shown in Eq. 3, where K_1 and K_2 are calibration constants.

$$LST = \frac{K_2}{\ln\left(\frac{K_1}{R} + 1\right)} \quad \text{(Eq.3)}$$

Where K_1 and K_2 are the calibration constants and R is the spectral radiance derived from previous step.

This two-step method calculates the LST based on brightness temperature, other popular algorithms with general higher accuracy including the Mono-Window Algorithm (Qin, Karnieli, and Berliner 2001) and Single-Channel Method (Jiménez-Muñoz et al. 2009). The more accurate LST value could be achieved by considering detailed land surface emissivity. However, the field data is incomplete in this study for some locations especially in the early stage of record. The term 'LST' used in this study is represented and based on at-satellite brightness which does not consider the effect from both surface emissivity and atmospheric correction parameter. Furthermore, the main focus in this study is to discover long-term trend and pattern, therefore land surface emissivity is assumed to be 1. To validate the relative accuracy of the LST results, the LST maps are compared to the weather stations' air temperature records from where different urban land-cover classes were corresponding. The UHI intensity was extracted based on annual and seasonal mean temperature.

4. Results and discussion

4.1. *Remotely sensed SUHI*

Figure 3 shows the seasonal UHI intensity from 1984 to 2014 by comparing urban area (downtown Toronto) with rural area (Beatrice). UHI intensity is quantified by average temperature difference between urban and rural sites. From the graph, the strongest UHI intensity mostly appears in the winter since 1984 with highest of 7.1°C in 2003. It is not surprising that the UHI intensity values in winter is generally stronger than traditional hot days in summer. The high latitude of the GTA increasing the need of heat supply during the winter which contributes the unique UHI phenomenon in the GTA. The seasonal UHI intensity did not present significant increasing trend like annual UHI intensity for the past 30 years in the GTA.

4.2. *Satellite derived LST*

The results of 1984 and 2014 SUHI intensity maps are shown and compared in Figure 4. The SUHI intensity was obtained by subtracting the lowest temperature in the map from the calculated LST. Red colour represents the degree of temperature difference. In areas under the strong SUHI phenomenon, the map will still show strong red colour even the temperature is low for that areas. This is the case in Figure 4 since the temperature associated withside map (24.3°C) on the right is lower than the map (26.1°C) on the left side. As shown in Figure 4, we could be conclude that the SUHI intensity is high in 2014 because widely distributed red areas

Figure 3. Seasonal UHI intensity (full line is urban area and dash line is rural area) from 1984 to 2014.

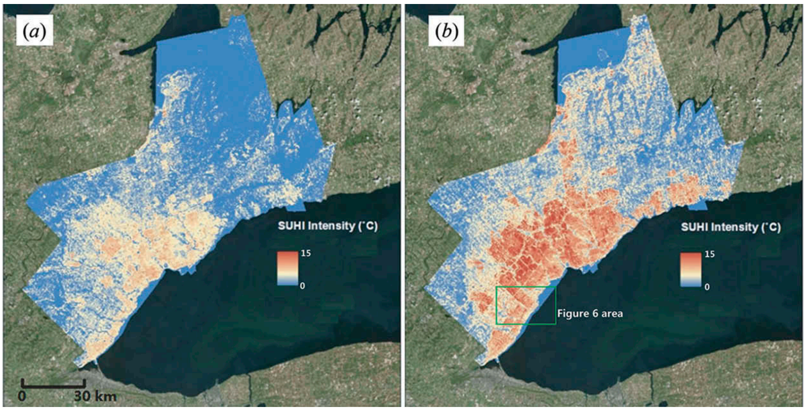

Figure 4. SUHI intensity map of the GTA in 1984(a) and 2014(b).

are shown on the SUHI intensity map of 2014. On the contrary, the map on the left showing very little red part that means the SUHI intensity is low in 1984.

4.3. SUHI characterization regarding to NDVI

The potential relationship between the normalized difference vegetation index(NDVI) and the LST is valuable when characterizing the SUHI in the GTA. Figure 5 shows the NDVI maps of the

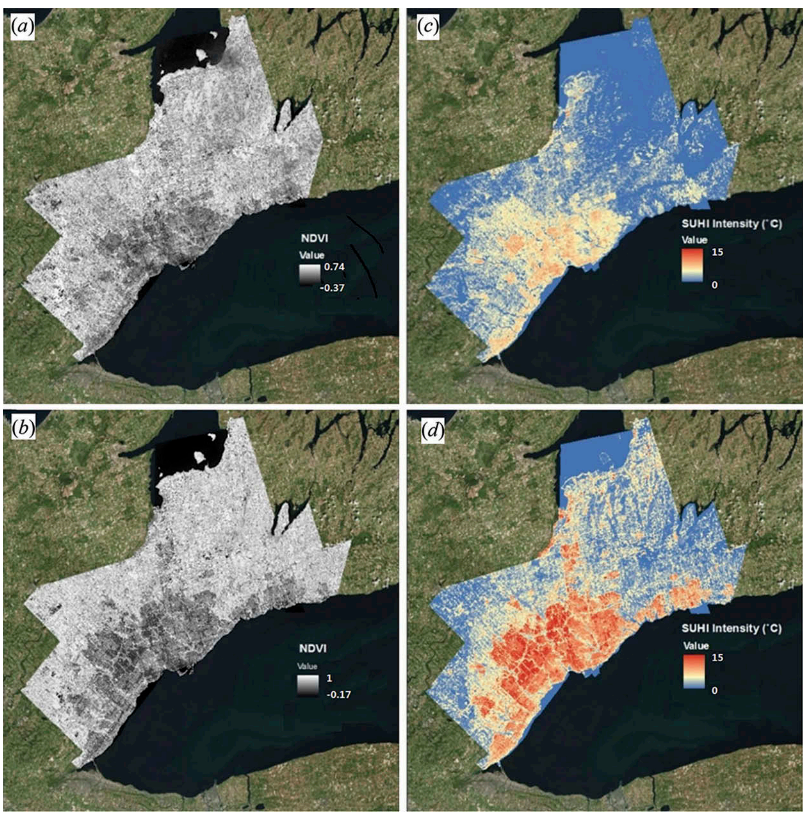

Figure 5. NDVI (1984:A,2014:B) and SUHI (1984:C,2014:D) intensity map of the GTA in 1984 and 2014.

GTA in 1984 and 2014,respectively. At the meantime, they are compared with the SUHI intensity for the corresponding year. As the urbanization effect, more and more green space is replaced by the built-up areas. The decreasing of the NDVI value and shrink of the vegetation extension are observed from the map on the left in Figure 5 with more black areas sprawled from the urban centre. The SUHI intensity is highlighted by red colour on the right of Figure 5. The increasing areas of the high SUHI intensity is agreeable with the growing areas with the low NDVI values, which shows the potential negative correlation from one to the other.

4.4. SUHI characterization regarding to land use

The shapfile of the land use classes of the GTA was integrated with the LST map to explore the underlying SUHI feature. The hot areas tend to distribute on central urban areas where the commercial and residential types of land use are highly centralized. Commercial areas typically have higher mean values of the LST compared to that of those parks. The possible explanations is that the commercial areas have a large amount of the impervious layers such as parking lots and building rooftops which absorb and store the heat, while parks are covered with vegetation or water which cools the surface by evaporation(see Figure 6)

Figure 6. Thermal behaviors of factories in LST map of the GTA.

4.5. SUHI characterization regarding to population

The SUHI is not only influenced by 'real' heat form but also can be shaped by the degree of human activities. Therefore, the population density as an indirect measure of the potential human activities could be connected with the SUHI characterization. The population density was classified into six classes in this study. The mean LST of each class was calculated based on the imagery acquired on August 27, 2011. Figure 7 shows the proportional relationship between the population density and the LST. Accordingly, it can be concluded that the population distribution affects the SUHI of the city by contributing to the increase of the LST.

4.6. SUHI characterization regarding to road network

The SUHI was characterized by considering transportation conditions in the GTA since many studies have suggested that the vehicle exhaust emission could promote the greenhouse gas emission which is acknowledged to be the primary contribution to the SUHI. Figure 8 shows the increasing of road coverage of the GTA from 2006 to 2014 by red lines and it combined with the LST map.

According to Figure 8, the LST enhances as the increasing of road network density. In allusion to the land use standpoint from the sections mentioned above, it is clear to conclude that the SUHI spreads from the city core. From another point of view, which is the viewpoint of road network, it is forceful to say that the SUHI extends along the main road network depends on its geographic appearance. The high traffic volume generates more heat than nearby low level streets.

5. Conclusions

In this study, the annual mean air temperature trend and characteristic of annual and seasonal UHI have been explored successfully in the GTA by analyzing the historical temperature records from local weather stations. Additionally, the long-term thermal band of satellite images have been applied to characterize the SUHI in the GTA regarding to different urban characteristics such as vegetation, land use, population and road network.

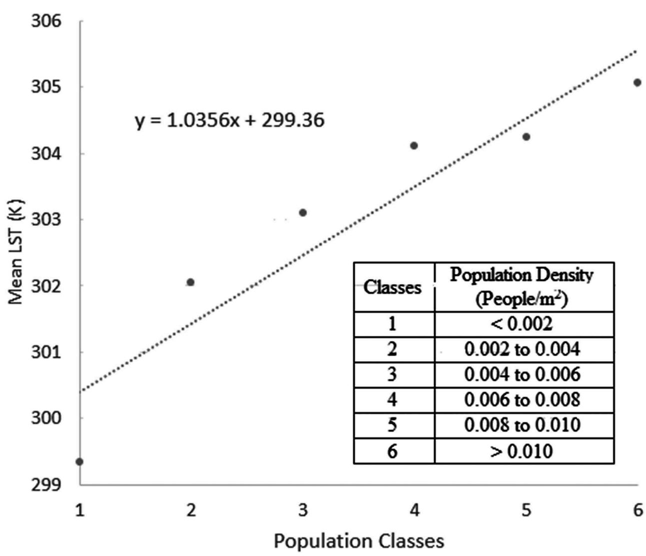

Classes	Population Density (People/m²)
1	< 0.002
2	0.002 to 0.004
3	0.004 to 0.006
4	0.006 to 0.008
5	0.008 to 0.010
6	> 0.010

Figure 7. Population density by classes vs. mean LST in 2011(Every class interval is 2000 persons/km^2 and class 1 is less than 2000 persons/km^2).

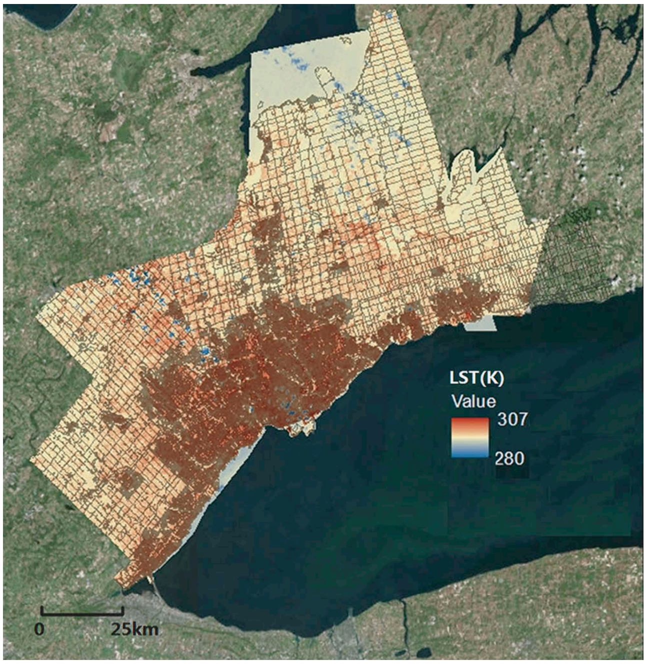

Figure 8. Overlay of the LST map on the road network of the GTA in 2014.

5.1. *Historical data trend*

The result of annual mean temperature trend test indicates a mild increasing trend for downtown Toronto and the very far rural weather stations. However, a significant increasing trend at 0.05 level for annual mean temperature is presented at the weather stations such as the Pearson International Airport and Richmond Hill where experiencing high pace development in recent decades. Despite the variation of significant level for air temperature trend at different locations, the annual UHI intensity of downtown Toronto is increased generally with increased extreme value during the past five years.

5.2. *SUHI mapping*

The result shows high correlation between image-based land surface temperature and weather stations' data, which implies the potential to convert LST to air temperature. After combining image-based LST map with NDVI, land use data, population density information and road network shapefile, SUHI is characterized accordingly. Finally, by connecting census data to LST, it shows directly connection between population density and LST in the GTA with high correlation coefficient.

Acknowledgements

The authors thank the National Key Research and Development Program of China (No. 2016YFB0502603), the National Natural Science Foundation of China (41001253), and Chinese Postdoctoral Science Foundation (2012M521717) for their support.

Funding

This work was supported by the National Key Research and Development Program of China; [2016YFB0502603]; National Natural Science Foundation of China; [41001253]; Chinese Postdoctoral Science Foundation; [2012M521717].

References

Coutts, A., J. Beringer, and N. Tapper. 2010. "Changing Urban Climate and CO(2) Emissions: Implications for the Development of Policies for Sustainable Cities." *Urban Policy and Research* 28 (1): 27–47. doi:10.1080/08111140903437716.

Curriero, F. C., K. S. Heiner, J. M. Samet, S. L. Zeger, L. Strug, and J. A. Patz. 2002. "Temperature and Mortality in 11 Cities of the Eastern United States." *American Journal of Epidemiology* 155 (1): 80–87. doi:10.1093/aje/155.1.80.

Dixon, P. G., and T. L. Mote. 2003. "Patterns and Causes of Atlanta's Urban Heat Island–Initiated Precipitation." *Journal of Applied Meteorology* 42 (9): 1273–1284. doi:10.1175/1520-0450(2003)042<1273:PACOAU>2.0.CO;2.

Finkenbine, J. K., J. W. Atwater, and D. S. Mavinic. 2000. "Stream Health after Urbanisation." *Journal of the American Water Resources Association* 36 (5): 1149–1160. doi:10.1111/j.1752-1688.2000.tb05717.x.

Jimenez-Munoz, J. C., J. Cristobal, J. A. Sobrino, G. Sòria, M. Ninyerola, and X. Pons. 2009. "Revision of the Single-Channel Algorithm for Land Surface Temperature Retrieval from Landsat Thermal-Infrared Data." *IEEE Transactions on Geoscience and Remote Sensing* 47 (1): 339–349. doi:10.1109/TGRS.2008.2007125.

Kat Snukal. 2014. "Toronto Star Series: Will Ontario's Future be Green?". http://www.greenbelt.ca/toronto_star_series_week6_future_2014

Krause, C. W., B. Lockard, T. J. Newcomb, D. Kibler, V. Lohani, and D. J. Orth. 2004. "Predicting Influences of Urban Development on Thermal Habitat in a Warm Water Stream." *Journal of the American Water Resources Association* 40 (6): 1645–1658. doi:10.1111/jawr.2004.40.issue-6.

Mohsin, T., and W. A. Gough. 2014. "Impact of Climate Change on the Extremes of Observed Daily Temperature Data in the Greater Toronto Area." *International Journal of Climate Change: Impacts and Responses* 5 (1): 11–33.

Qin, Z., A. Karnieli, and P. Berliner. 2001. "A Mono-Window Algorithm for Retrieving Land Surface Temperature from Landsat TM Data and Its Application to the Israel-Egypt Border Region." *International Journal of Remote Sensing* 22 (18): 3719–3746. doi:10.1080/01431160010006971.

Rosenfeld, A. H., H. Akbari, S. Bretz, B. L. Fishman, D. M. Kurn, D. Sailor, and H. Taha. 1995. "Mitigation of Urban Heat Islands: Materials, Utility Programs, Updates." *Energy and Buildings* 22 (3): 255–265. doi:10.1016/0378-7788(95)00927-P.

Scott, R. W., and F. A. Huff. 1996. "Impacts of the Great Lakes on Regional Climate Conditions." *Journal of Great Lakes Research* 22 (4): 845–863. doi:10.1016/S0380-1330(96)71006-7.

Semenza, J. C., C. H. Rubin, K. H. Falter, J. D. Selanikio, W. D. Flanders, H. L. Howe, and J. L. Wilhelm. 1996. "Heat-Related Deaths during the July 1995 Heat Wave in Chicago." *The New England Journal of Medicine* 335 (2): 84–90. doi:10.1056/NEJM199607113350203.

Smargiassi, A., M. Fournier, C. Griot, Y. Baudouin, and T. Kosatsky. 2008. "Prediction of the Indoor Temperatures of an Urban Area with an In-Time Regression Mapping Approach." *Journal of Exposure Science & Environmental Epidemiology* 18 (3): 282–288. doi:10.1038/sj.jes.7500588.

Sobrino, J. A., R. Oltra-Carrió, G. Sòria, J. C. Jiménez-Muñoz, B. Franch, V. Hidalgo, and M. Paganini. 2013. "Evaluation of the Surface Urban Heat Island Effect in the City of Madrid by Thermal Remote Sensing." *International Journal of Remote Sensing* 34 (9–10): 3177–3192.